JOC The Journal of Organic Chemistry

Article

pubs.acs.org/joc

Theoretical Analysis of Reactivity Patterns in Diels–Alder Reactions of Cyclopentadiene, Cyclohexadiene, and Cycloheptadiene with Symmetrical and Unsymmetrical Dienophiles

Brian J. Levandowski and K. N. Houk*

Department of Chemistry and Biochemistry, University of California, Los Angeles, California 90095, United States

Supporting Information

ABSTRACT: The Diels–Alder reactions of cyclopentadiene, cyclohexadiene, and cycloheptadiene with a series of dienophiles were studied with quantum mechanical calculations (M06-2X density functional theory) and analyzed with the distortion/interaction model. The poor reactivities of cyclohexadiene and cycloheptadiene with dienophiles that give relatively synchronous transition states result from the substantial distortion required to achieve a transition state involving the formation of two bonds of the diene simultaneously. However, highly asynchronous or stepwise reactions result in less distortion of the diene and less differences in reactivities of different dienes. The transition state geometry of cyclopentadiene is less distorted in the asynchronous reaction with 1,1-dicyanoethylene compared to that with *cis*- and *trans*-1,2-dicyanoethylenes, which react through synchronous transition states.

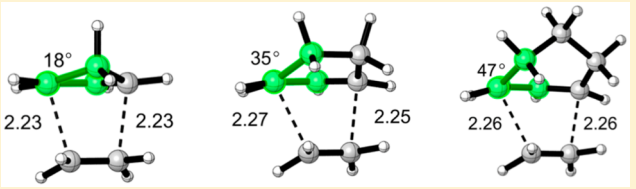

INTRODUCTION

The high reactivities of cyclopentadienes in the Diels–Alder reaction have led to applications including organic synthesis,[1] biomolecule immobilization,[2] thermally sensitive polymers,[3] and the functionalization[4] of materials. Cyclohexadiene and cycloheptadiene are less reactive and less useful in such applications. A SciFinder[5] search for Diels–Alder reactions of cyclopentadiene, cyclohexadiene, and cycloheptadiene gave ~5000 reactions involving cyclopentadiene, ~1500 with cyclohexadiene, and only ~70 with cycloheptadiene.

The poor reactivity of cyclohexadiene and cycloheptadiene relative to that of cyclopentadiene with cyclobutenone was recently reported by Danishefsky and computationally investigated by our lab (Scheme 1).[6]

The experimentally determined HOMO energies of the cyclic dienes range only from −8.6 to −8.3 eV.[7,8] If the frontier molecular orbitals governed the reactivity, then similar reactivities would be expected for all three cyclic dienes. The computed transition state barriers, however, show that, with cyclobutenone, cyclopentadiene is about 100 times more reactive than cyclohexadiene and about 15 000 times more reactive than cycloheptadiene, at 298 K.[6] We have shown that the reactivity is controlled by distortion energies: cyclopentadiene requires only 15.0 kcal/mol to distort into the transition state geometry, which is 4.2 kcal/mol less than that for cyclohexadiene and 7.1 kcal/mol less than that for cycloheptadiene.

The hetero-Diels–Alder reactions of both *N*-phenyl-1,2,4-triazolin-3,5-dione (PTAD) and nitrosobenzene with all three cyclic dienes, however, occur readily under mild conditions, as shown in Scheme 2.[9−13]

Scheme 1. Diels–Alder Reactions of Cyclobutenone with the Three Cyclic Dienes[6]

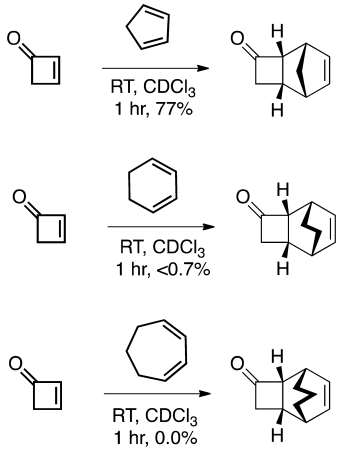

The Diels–Alder reactions of cyclopentadiene with PTAD and nitrosobenzene occur at 0 °C (Scheme 2a,d). Cyclohexadiene reacts with nitrosobenzene (Scheme 2e) and a cyclohexadiene derivative reacts with PTAD (Scheme 2b) at 0 °C with comparable yields to the corresponding reactions with cyclopentadiene. At room temperature, a cycloheptadiene derivative is reactive with both PTAD and nitrosobenzene (Scheme 2c,f). Unlike the reactions with cyclobutenone, the reactions of the cyclic dienes with PTAD and nitrosobenzene

Received: January 23, 2015
Published: March 5, 2015

DOI: 10.1021/acs.joc.5b00174
J. Org. Chem. 2015, 80, 3530−3537

Scheme 2. Diels–Alder Reactions of PTAD and Nitrosobenzene with the Three Cyclic Dienes

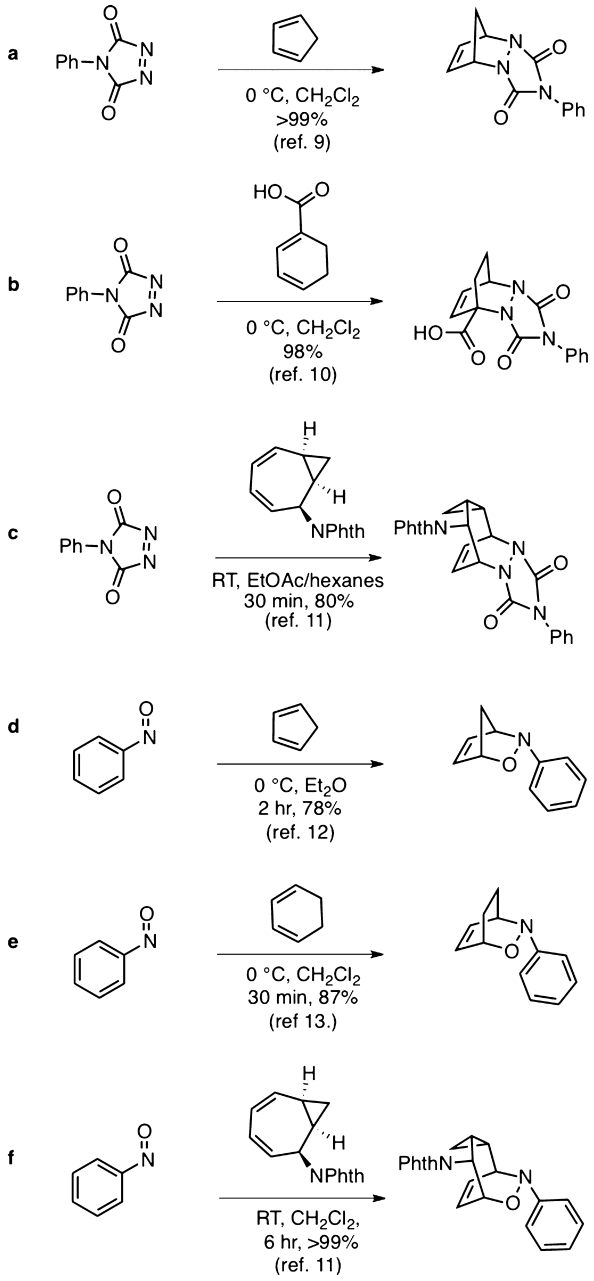

occur under similar conditions, with a cycloheptadiene derivative being only modestly less reactive.

Cyclic dienes are more reactive than acyclic dienes in Diels–Alder reactions, in part because they are locked into the s-*cis* conformation required of concerted Diels–Alder transition states.[14] To rationalize the poor reactivities of cyclohexadiene and cycloheptadiene relative to that of cyclopentadiene in the Diels–Alder reaction, it has been proposed that the steric interactions between the bridges of cyclohexadiene and cycloheptadiene result in repulsive steric interactions with the dienophile and inhibit the double bonds from adopting the necessary planar geometry in the transition state.[15] Correlations between the diene 1,4-distance and the reactivity of dienes identify an additional factor controlling the high reactivity of cyclopentadiene and poor reactivity of cycloheptatriene with dienophiles.[16] That is, the termini of cyclopentadiene are closer together than termini of acyclic dienes, whereas in cycloheptatriene the termini are fixed further apart. These models explain why dienophiles such as maleic anhydride readily react with anthracene and show no reactivity with 1,3-cyclooctadiene.[17] Nitrosobenzene, however, reacts with 1,3-cyclooctadiene and fails to react with anthracene even after prolonged reflux in chloroform.[17]

We have studied the origins of reactivity differences between cyclic dienes of different ring sizes and show why dienophiles like *N*-phenyl-1,2,4-triazolin-3,5-dione and nitrosobenzene have similar reactivities toward the three cyclic dienes. We theoretically investigated the reactivities of cyclic dienes (**1**–**3**) with dienophiles, ethylene (**A**), methyl vinyl ketone (MVK, **B**), *N*-phenyl-1,2,4-triazolin-3,5-dione (PTAD, **C**), and nitrosobenzene (**D**). We also included the cyanoethylenes (**E**–**J**) previously studied experimentally by Sauer[18] (Chart 1) as well as used in a number of theoretical studies.[19,20]

Chart 1. Dienes 1–3 and Dienophiles A–J

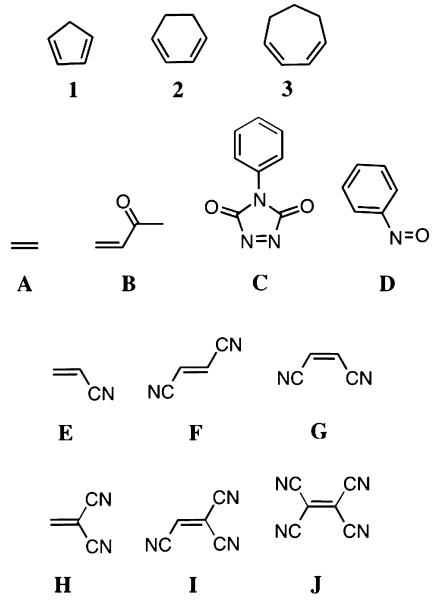

COMPUTATIONAL METHODS

Computations were carried out with *Gaussian 09*, Revision D.01.[21] Geometry optimizations and frequency calculations were performed using the M06-2X[22] density functional with the 6-31+G(d) basis set. The M06-2X functional is known to reproduce the free energies of cycloadditions better than other functionals.[23] Single-point energies were evaluated using the 6-311++G(d,p) basis set. Solvation effects of dichloromethane (DCM) for the reactions of **A**–**D** and 1,4-dioxane for the reactions of **E**–**J** with cyclic dienes **1**–**3** were included in the optimizations and single-point energies by the self-consistent reaction field (SCRF) using the CPCM model.[24,25] Normal mode analysis of each structure verified that each stationary point is either a first-order saddle point or a minimum. The thermal corrections were computed from unscaled M06-2X/6-31+G(d) frequencies for a standard state of 1 M and 298.15 K.

RESULTS AND DISCUSSION

The transition structures of the cycloadditions involving dienes **1**–**3** and dienophiles **A**–**D** are shown in Figure 1.

In the reactions of ethylene, MVK, and PTAD with the three cyclic dienes, the activation free energies increase from cyclopentadiene to cycloheptadiene. The activation free

DOI: 10.1021/acs.joc.5b00174
J. Org. Chem. 2015, 80, 3530–3537

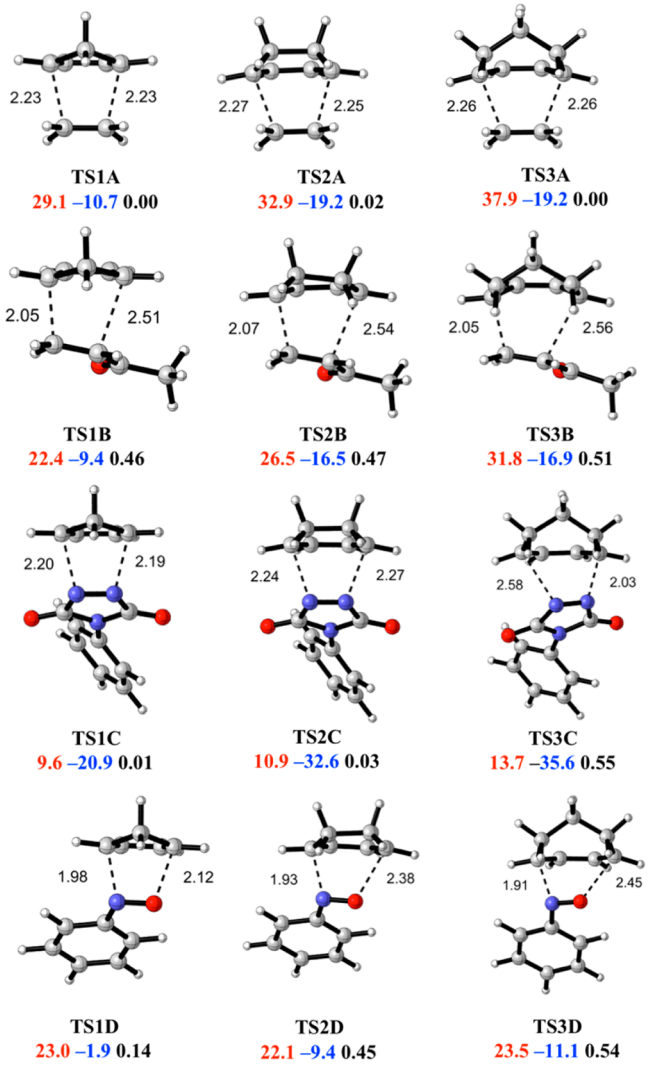

Figure 1. M06-2X/6-31+G(d) transition structures for the reactions of dienes **1**–**3** with dienophiles **A**–**D**. The forming bond lengths are reported in angstroms (red, activation free energy ($\Delta G^{\ddagger}$, kcal/mol); blue, reaction free energy (ΔG, kcal/mol); black, asynchronicity ($\Delta r^{\ddagger}$, angstroms)).

energies for the reactions of cyclopentadiene with ethylene and MVK are 29.1 and 22.4 kcal/mol, respectively. The barriers increase to 32.9 and 26.5 kcal/mol with cyclohexadiene and to 37.9 and 31.8 kcal/mol with cycloheptadiene. With PTAD, the reactivity differences are smaller. The activation free energy of cyclopentadiene with PTAD is 9.6 kcal/mol. With cyclohexadiene and cycloheptadiene, the barriers with PTAD are 10.9 and 13.7 kcal/mol, respectively. The activation free energies for the reactions of nitrosobenzene with the three cyclic dienes are comparable, ranging from 22.1 to 23.5 kcal/mol. The computed rate constants for the reactions of the three cyclic dienes span 6 orders of magnitude with ethylene and MVK, 3 orders of magnitude with PTAD, and 1 order of magnitude with nitrosobenzene.

The transition states are all concerted but with varying degrees of asynchronicity. The transition states involving ethylene **TS(1**–**3)A** are all nearly synchronous, with $\Delta r^{\ddagger}$ = 0.02 Å at most. The reactions of PTAD with cyclopentadiene **TS1C** and cyclohexadiene **TS2C** proceed through approximately synchronous transition structures, whereas the reaction with cycloheptadiene **TS3C** occurs through a highly asynchronous transition structure. The transition structures for the reactions of the cyclic dienes with unsymmetrical dienophiles, MVK **TS(1**–**3)B** and nitrosobenzene **TS(1**–**3)D**, are all asynchronous. The asynchronicity of the transition structures increases from cyclopentadiene to cycloheptadiene for the reactions of MVK ($\Delta r^{\ddagger}$ = 0.46–0.51 Å), PTAD ($\Delta r^{\ddagger}$ = 0.01–0.55 Å), and nitrosobenzene ($\Delta r^{\ddagger}$ = 0.14–0.54 Å). The reactions of cyclohexadiene and cycloheptadiene are 7–15 kcal/mol more exothermic than the reactions of cyclopentadiene. Consistent with the Hammond postulate, the transition structures of cyclohexadiene and cycloheptadiene are earlier than with cyclopentadiene.

The distortion/interaction (or activation strain) model was applied in order to determine the origins of these differences in reactivity.[26] When applied to the intermolecular Diels–Alder reactions studied here, this model dissects the activation energy into the energies required to distort the diene ($\Delta E^{\ddagger}_{\mathrm{d-diene}}$) and the dienophile ($\Delta E^{\ddagger}_{\mathrm{d-dienophile}}$) into the transition state geometry without allowing them to interact and the interaction energy ($\Delta E^{\ddagger}_{\mathrm{i}}$), which is the difference between the total distortion energy ($\Delta E^{\ddagger}_{\mathrm{d}} = \Delta E^{\ddagger}_{\mathrm{d-diene}} + \Delta E^{\ddagger}_{\mathrm{d-dienophile}}$) and the activation energy ($\Delta E^{\ddagger}$).

Trends in activation enthalpies ($\Delta H^{\ddagger}$) are often described in terms of the relative heat of reactions (ΔH_{rxn}). Such correlations are known as BEMA HAPOTHLE relationships developed from insight by Bell, Marcus, Hammond, Polanyi, Thornton, and Leffler to explain and rationalize linear free energy relationships.[27] As shown in Figure 2, the activation enthalpies for the cycloadditions involving cyclic dienes do not correlate with the reaction enthalpies, whereas there is a better, if still rough, correlation between the activation energies and distortion energies. This modest correlation is a result of a wide range of interaction energies, from −5.5 to −20.9 kcal/mol, associated with the very different electronic properties of the dienophiles studied.

Figure 3 shows the distortion/interaction analysis for the Diels–Alder reactions of the cyclic dienes **1**–**3** with dienophiles **A**–**D**.

For a given dienophile, the distortion energies of the dienophile are nearly constant to within 1–2 kcal/mol. The distortion energies of the dienes increase from 15.9 to 22.6 kcal/mol as the diene changes from cyclopentadiene to cycloheptadiene with ethylene **TS(1**–**3)A** and from 13.5 to 19.5 kcal/mol with MVK **TS(1**–**3)B**. The increases in the diene distortion energies parallel the increases in the activation energies among the cyclic dienes with ethylene and MVK. MVK is a more reactive dienophile than ethylene because it has stronger interaction energies and smaller diene distortion energies, the latter being a result of the asynchronous transition structures that we will discuss later.

PTAD and nitrosobenzene show similar reactivities toward the three cyclic dienes because the differences in diene distortion are small. In the highly asynchronous transition state **TS3C** (0.54 Å), the diene distortion energy of cycloheptadiene is 12.5 kcal/mol, only 1.4 kcal/mol higher than that for cyclopentadiene **TS1C** and 1.9 kcal/mol lower than that for cyclohexadiene **TS2C**. For nitrosobenzene, the distortion energy of cycloheptadiene **TS3D** is 14.9 kcal/mol, 1.3 kcal/mol lower than that for cyclopentadiene **TS1D** and 1.7 kcal/mol lower than that for cyclohexadiene **TS2D**.

The interaction energies are nearly constant in reactions of the cyclic dienes with ethylene and MVK. However, the

DOI: 10.1021/acs.joc.5b00174
J. Org. Chem. 2015, 80, 3530–3537

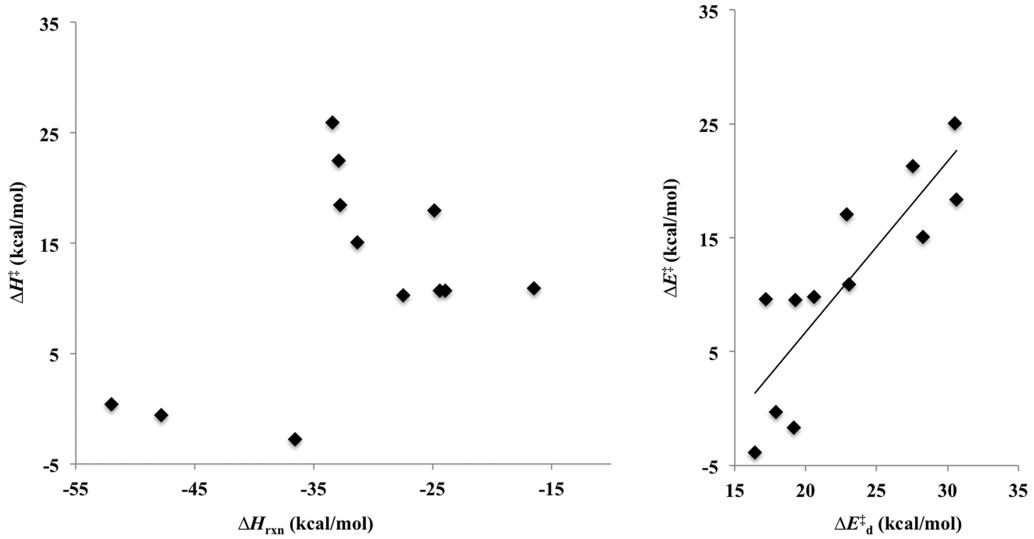

Figure 2. Plots of activation enthalpy ($\Delta H^{‡}$) versus enthalpy of reaction (ΔH_{rxn}) (left, r^2 = 0.21, $\Delta H^{‡}$ = 0.42ΔH_{rxn} + 25.0) and the activation energy ($\Delta E^{‡}$) versus distortion energy ($\Delta E^{‡}_{d}$) (right, r^2 = 0.73, $\Delta E^{‡}$ = 1.50$\Delta E^{‡}_{d}$ − 23.2) for the reactions of cyclic dienes **1**−**3** with dienophiles **A**−**D**.

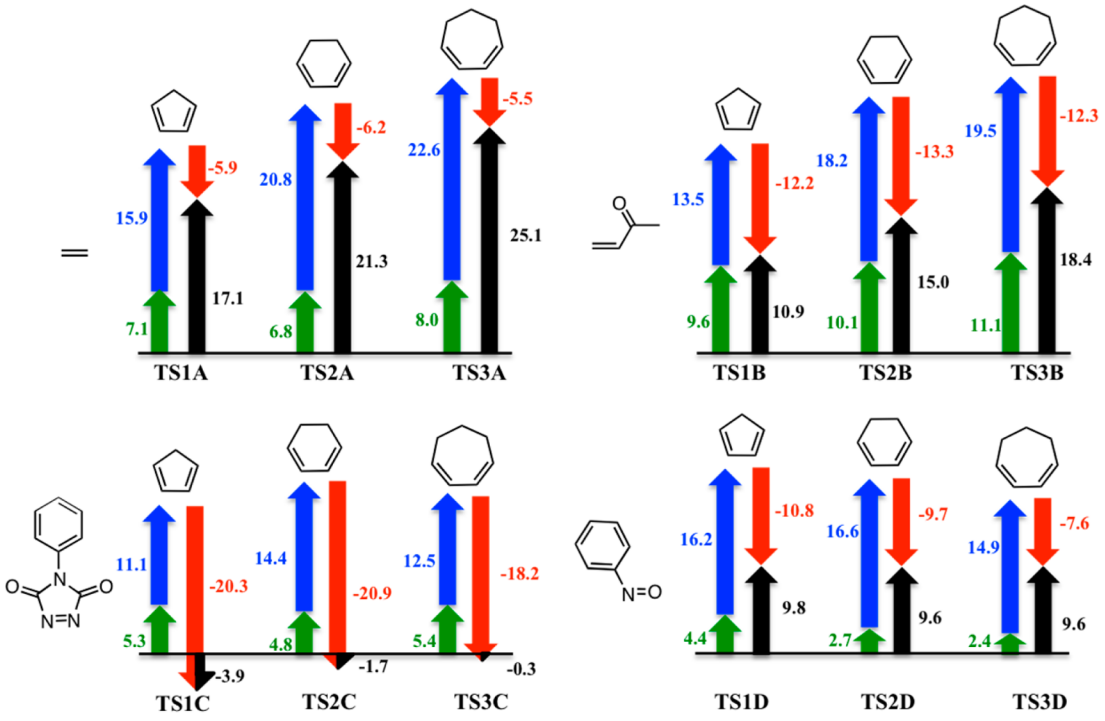

Figure 3. Plots of the distortion, interaction, and activation energies for the transition states involving dienophiles **A**−**D** and cyclic dienes **1**−**3** (green, distortion energy of dienophile; blue, distortion energy of diene; red, interaction energy; black, activation energy; in kcal/mol).

interaction energies decrease in the reactions involving PTAD and nitrosobenzene as the asynchronicity of the reaction increases. The interaction energy for the asynchronous transition structure of **TS3C** is lower than that of the synchronous transition states **TS1C** and **TS2C** by 2.1 and 2.7 kcal/mol, respectively. For the nitrosobenzene series, the interaction energies decreases from −10.8 kcal/mol with cyclopentadiene to −9.7 and −7.6 kcal/mol with cyclohexadiene and cycloheptadiene, respectively. This trend corresponds with the increase in asynchronicity, which results in similar diene distortion energies and decreasing interaction energies.

The distortion of each diene is associated with the pyramidalization of the diene termini required in order to form both new bonds simultaneously. Pyramidalization enables overlap of the hybrid orbitals at the diene termini with the π orbitals at the termini of the dienophile. As the dienophile approaches, the diene distorts from planarity at the termini of the C_1C_2 and C_3C_4 double bonds of the diene. This distortion unfavorably reduces the C_1C_2 and C_3C_4 π overlap. The dihedral angles θ_1 and θ_2, across the C_1C_2 and C_3C_4 diene double bonds, measure the out-of-plane distortion of the carbon atoms in the diene bridge directly attached to the double bond. Figure 4 shows θ_1 in the transition structures for the reactions of ethylene with the cyclic dienes.

DOI: 10.1021/acs.joc.5b00174
J. Org. Chem. 2015, 80, 3530−3537

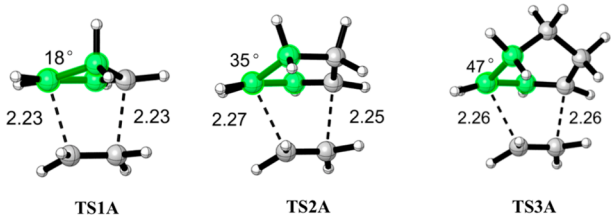

Figure 4. Nearly synchronous Diels–Alder transition structures of cyclic dienes, **1**–**3**, with ethylene, showing dihedral angle θ_1 that measures the out-of-plane distortion along the C_1C_2 double bond of the diene. The highlighted atoms define θ_1.

The increase in diene distortion energy from cyclopentadiene to cycloheptadiene in the nearly synchronous transition structures, **TS1A** to **TS3A**, results from the increase in the out-of-plane distortion across the C_1C_2 and C_3C_4 double bonds in the transition structures. The difference in the transition state structures is reflected in the geometry of the Diels–Alder adducts (Figure 5). With a longer diene bridge, θ_1 and θ_2 increase to minimize ring strain in the tether connecting C_1 to C_4.

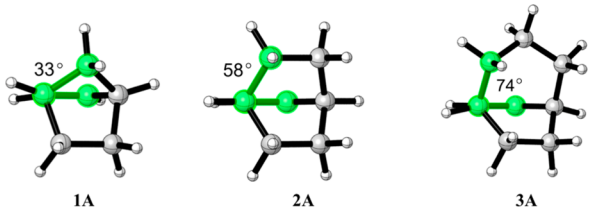

Figure 5. Diels–Alder adducts from the reactions of ethylene with cyclic dienes, **1**–**3**, showing dihedral angle θ_1.

Figure 6 shows for the nearly synchronous transition structures with ethylene **TS(1–3)A** that the out-of-plane distortion is the same on each side of the diene such that $\theta_1 = \theta_2$. For asynchronous transition structures **TS(1–3)D**, the dihedral angle associated with the lesser-formed C–O bond is less distorted from the plane of the diene than the dihedral angle associated with the forming C–N bond.

The sum of θ_1 and θ_2 ($\sum(\theta_1 + \theta_2)$) and the diene distortion energies for the synchronous reaction **TS1A** and the asynchronous reaction **TS1D** are nearly identical at 36° and 15.9 kcal/mol and 35° and 16.2 kcal/mol, respectively. For the reactions with cyclohexadiene, the $\sum(\theta_1 + \theta_2)$ is 70° for **TS2A** and the diene distortion energy is 20.8 kcal/mol compared to that of **TS2D**, where the $\sum(\theta_1 + \theta_2)$ is only 58° and the diene distortion energy is only 16.6 kcal/mol. For the reactions with cycloheptadiene, the $\sum(\theta_1 + \theta_2)$ is 94° and the diene distortion energy is 22.6 kcal/mol in the synchronous reaction **TS3A** compared to that for the highly asynchronous **TS3D**, where the $\sum(\theta_1 + \theta_2)$ is only 74° and the diene distortion energy is only 14.9 kcal/mol.

Figure 7 shows the energetic cost for the out-of-plane distortion about the double bond of dienes **1**–**3**, 1,3-butadiene, and 1,3-cyclooctadiene.

The shorter rigid bridges of cyclopentadiene and cyclohexadiene restrict the out-of-plane motion, resulting in a substantial increase in the force constants associated with the out-of-plane distortion. The 3- and 4-atom bridges of cycloheptadiene and cyclooctadiene are flexible enough that the force constants for the out-of-plane motion are similar to the model acyclic diene, 1,3-butadiene.

Having established the role of asynchronicity in the reactivity of cyclic dienes, we revisited the classic Sauer[18] rate constants for the reactivities of cyclopentadiene with cyanoethylenes **E**–**J**. The nature of the transition states of these and other Diels–Alder reactions have been explored in many prominent studies,[19] most recently by Politzer, Murray, and co-workers.[20] They analyzed the asynchronicity of transition states of unsymmetrically substituted dienophiles, using the force constants along the reaction pathway, and found that highly asynchronous processes have two minima of the second

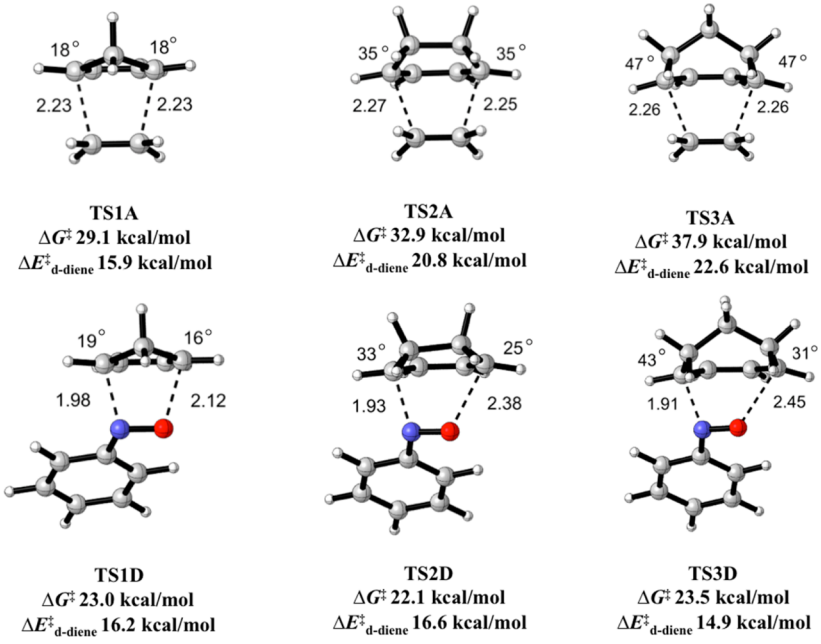

Figure 6. Transition structures for the reactions of dienes **1**–**3** with dienophiles **A** and **D** showing dihedral angle θ_1 across the C_1C_2 diene double bond and dihedral angle θ_2 across the C_3C_4 diene double bond.

DOI: 10.1021/acs.joc.5b00174
J. Org. Chem. 2015, 80, 3530–3537

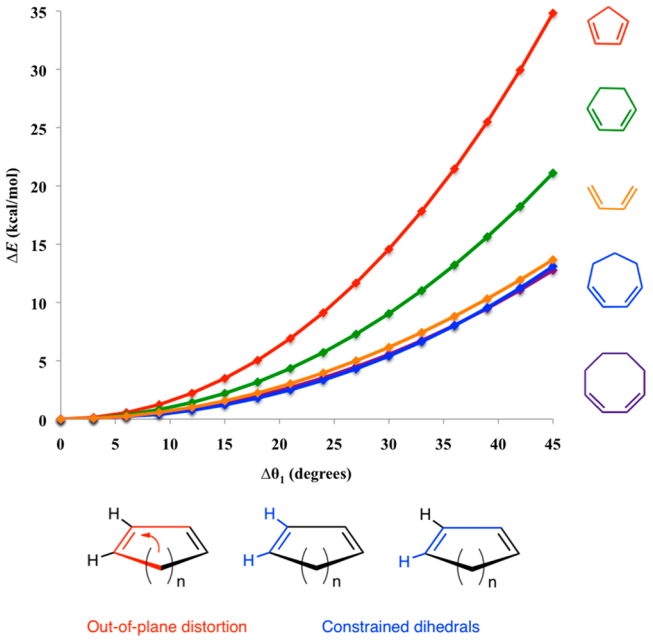

Figure 7. M06-2X/6-31+G(d)/CPCM(DCM) deformation energy (relative to fully optimized cyclic diene) for the out-of-plane motion ($\Delta\theta_1$) across the C_1C_2 double bond of dienes **1**−**3**, 1,3-butadiene, and 1,3-cyclooctadiene from 0° to 45° in 5° increments.

derivative in the transition region, indicative of a stepwise formation of bonds even in the absence of an energetic intermediate.[20a] They also analyzed these reactions in terms of an electron density analysis[20b] and electrostatic potentials.[20c]

The experimental rate constants for the reactions of cyclopentadiene with the cyanoethylenes are summarized in Table 1 along with the computed activation free energies.

Table 1. Experimental Rate Constants and Calculated Activation Energies for the Reactions of Cyclopentadiene with Ethylene and Cyanoethylenes E−J

dienophile	log k_{exp} [M^{-1} s^{-1}]	$\Delta G^{\ddagger}_{calc}$ (kcal/mol, 298 K)
ethylene (**TS1A**)	1.9[a]	29.1
acrylonitrile (**TS1E-*endo***)	5.0[b]	21.8
fumaronitrile (**TS1F**)	5.9[b]	16.8
maleonitrile (**TS1G-*endo***)	6.0[b]	16.2
vinylidene cyanide (**TS1H**)	9.7[b]	12.5
tricyanoethylene (**TS1I-*endo***)	10.7[b]	9.6
tetracyanoethylene (**TS1J**)	12.6[b]	5.9

[a]Adjusted to 293 K from ref 28. [b]Dioxane, 293 K; see ref 18.

Figure 8 shows a comparison of the M06-2X computed activation free energies ($\Delta G^{\ddagger}_{calc}$) and the log of the experimental rate constants. Previous studies have shown that the B3LYP functional poorly predicts the substituent effects for the reactions of tricyanoethylene and tetracyanoethylene with cyclopentadiene.[19k−m] The M06-2X functional predicts the correct reactivity pattern for the differently substituted cyanoethylenes.

Both the experimental rates and computed activation barriers show that the reactivity increases with the number of electron-withdrawing cyano substituents. The reason why 1,1-dicyanoethylene is 500 times more reactive than the *cis*- and *trans*-1,2-dicyanoethylene, as well as a theoretical explanation of all of these data, has been the focus of numerous computational studies.[19]

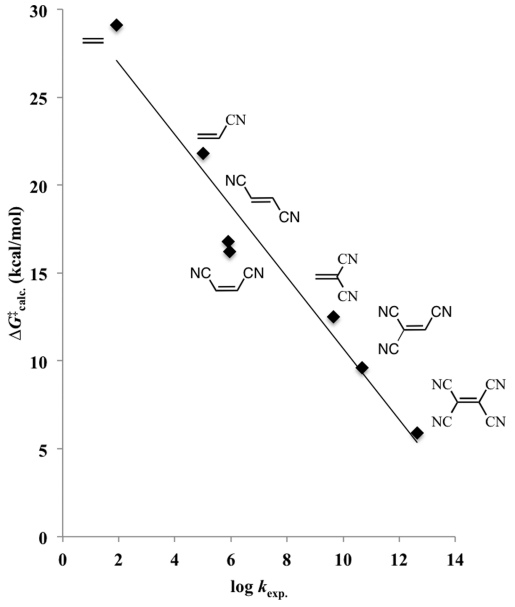

Figure 8. Plot of computed activation free energies (298 K) vs log k_{exp} (r^2 = 0.95, $\Delta G^{\ddagger}_{calc}$ = −2.0 log k_{exp} + 31.0).

Figure 9 shows the distortion/interaction analysis of these reactions. The difference in the reactivity between the unsymmetrically and symmetrically substituted dienophiles is related to both the energy required to distort cyclopentadiene and the interaction energy that has been discussed previously in terms of FMO interactions between the reactants.

For the reactions of cyclopentadiene with ethylene **A** and cyanoethylenes **E**−**J**, the activation free energies range from 29.1 to 5.9 kcal/mol. The different reactivities along the series of dienophiles with cyclopentadiene results from increases in interaction energies as the number of cyano substituents on the dienophile increases. Figure 10 shows an excellent linear correlation of the transition state interaction energies with the number of cyano substituents.

The interaction energies range from −5.9 to −30.0 kcal/mol and become 1−11 kcal/mol stronger with each additional cyano substituent.

The diene distortion energy for the reactions of cyclopentadiene with **A** and cyanoethylenes **E**−**J** ranges from 11.7 to 15.9 kcal/mol. Figure 11 shows an excellent linear relation between the diene distortion energy and the $\sum(\theta_1 + \theta_2)$, discussed earlier.

The diene distortion energies increase as the out-of-plane distortion from the C_1C_2 and C_3C_4 double bonds increases. The range, however, is small in the context of the interaction energies, with only a 4.2 kcal/mol difference at most. The high reactivity of dicyanoethylenes is mainly due to the interaction energies, but the 500-fold increase in reactivity of 1,1-dicyanoethylene relative to that of the *cis*- and *trans*-1,2-dicyanoethylenes is a result of the asynchronous transition state with the former. The 2.4−3.0 kcal/mol lower cyclopentadiene distortion energy of the transition state with 1,1-dicyanoethylene is because only one terminus of the diene is distorted appreciably. This is a result of a less fully formed C−C bond (2.65 Å) in **TS1H** and less distortion about the double bonds than that in the synchronous transitions states **TS1F** and **TS1G**.

DOI: 10.1021/acs.joc.5b00174
J. Org. Chem. 2015, 80, 3530−3537

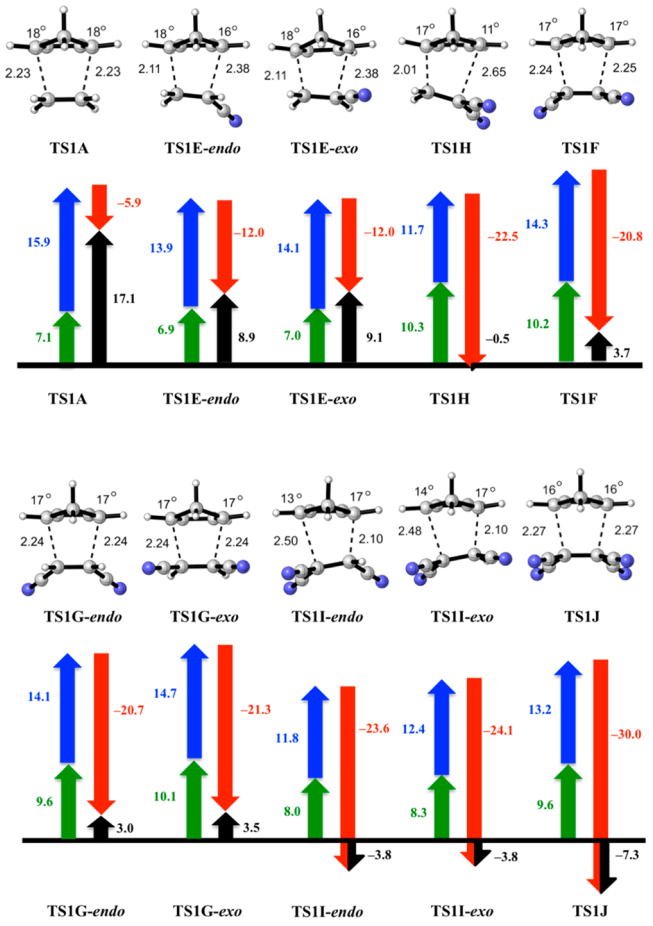

Figure 9. Optimized transition structures for reactions of cyclopentadiene with dienophiles **A** and **E**–**J**. The forming bond lengths are reported in angstroms, and dihedral angles for θ_1 and θ_2 are reported in degrees. Distortion, interaction, and activation energies for the transition structures are shown below each structure (green, distortion energy of dienophile; blue, distortion energy of diene; red, interaction energy; black, activation energy; in kcal/mol).

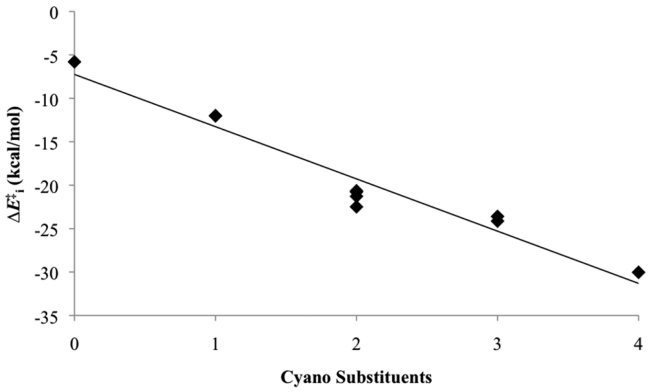

Figure 10. Plot of the interaction energy for the reactions of cyclopentadiene with dienophiles **A** and **E**–**J** vs the number of cyano substituents (r^2 = 0.94, $\Delta E^{\ddagger}_{i} = 6.0x - 7.3$).

CONCLUSIONS

The out-of-plane distortion across the C_1C_2 and C_3C_4 diene double bonds has a significant impact on the Diels–Alder reactivities of cyclic dienes. Cyclopentadiene is highly reactive in Diels–Alder reactions because only minimal out-of-plane distortion is required to achieve the transition state geometry compared with that of other cyclic and acyclic dienes. Asynchronous transition states have significant out-of-plane distortion about only one double bond. With heterodienophiles, such as nitrosobenzene and PTAD, the asynchronicity of the transition states results in similar reactivities for all three cyclic dienes.

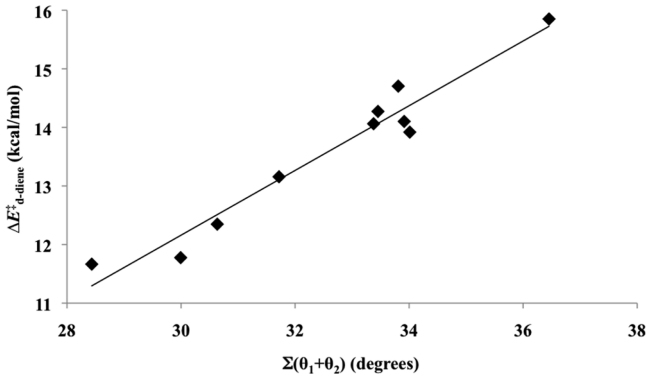

Figure 11. Plot of the diene distortion energy for the reactions of cyclopentadiene with dienophiles **A** and **E**–**J** against $\sum(\theta_1 + \theta_2)$ (r^2 = 0.95, $\Delta E^{\ddagger}_{d-diene} = 0.55 \sum(\theta_1 + \theta_2) - 4.4$).

ASSOCIATED CONTENT

Supporting Information

Cartesian coordinates and energies of all optimized structures and transition structures. This material is available free of charge via the Internet at http://pubs.acs.org.

AUTHOR INFORMATION

Corresponding Author

*E-mail: houk@chem.ucla.edu.

Notes

The authors declare no competing financial interest.

ACKNOWLEDGMENTS

We are grateful to the National Science Foundation (CHE-1449755) for financial support of the research. We thank Steven Lopez and Dr. Yu-hong Lam for helpful discussions. We also thank the University of California Los Angeles IDRE for use of the Hoffman 2. We thank Prof. Claude Y. Legault for CYLview,[29] which was used to generate images of the optimized structures.

REFERENCES

(1) (a) Wyvratt, M. J.; Paquette, L. A. *J. Am. Chem. Soc.* **1974**, *96*, 4671. (b) Kentgen, G.; Balogh, W. D.; Ternansky, R. J.; Paquette, L. A. *J. Am. Chem. Soc.* **1983**, *105*, 5446. (c) Shi, Y.; Wilmot, J. T.; Nordstrøm, L. U.; Tan, D. S.; Gin, D. Y. *J. Am. Chem. Soc.* **2013**, *135*, 14313.

(2) Kron, J. S.; Huh, J. H.; Mrksich, M.; Houseman, B. T. *Nat. Biotechnol.* **2002**, *20*, 270.

(3) Samoshin, A. V.; Hawker, C. J.; de Alaniz, J. R. *ACS Macro. Lett.* **2014**, *3*, 753.

(4) Bian, S.; Scott, A. M.; Cao, Y.; Liang, Y.; Osuna, S.; Houk, K. N.; Braunschweig, A. B. *J. Am. Chem. Soc.* **2013**, *135*, 9240.

(5) SciFiner. https://scifinder.cas.org.

(6) Paton, R. S.; Kim, S. K.; Ross, A. G.; Danishefsky, S. J.; Houk, K. N. *Angew. Chem., Int. Ed.* **2011**, *50*, 10366.

(7) Worley, S. D.; Dewar, M. J. S. *J. Chem. Phys.* **1968**, *49*, 2454.

(8) Bischof, P.; Heilbronner, E. *Helv. Chim. Acta* **1970**, *53*, 1677.

DOI: 10.1021/acs.joc.5b00174
J. Org. Chem. 2015, 80, 3530–3537

(9) Perez Luna, A.; Ceschi, M. A.; Bonin, M.; Micouin, L.; Husson, H. P. *J. Org. Chem.* **2002**, *67*, 3522.
(10) Hennig, A.; Schwarlose, T.; Nau, W. N. *ARKIVOC* **2007**, *8*, 341.
(11) Templin, S. S.; Wallock, N. J.; Bennett, D. W.; Siddiquee, T.; Haworth, D. T.; Donaldson, W. A. *J. Heterocycl. Chem.* **2007**, *44*, 719.
(12) Kresze, G.; Schulz, G. *Tetrahedron* **1961**, *12*, 7.
(13) Yang, B.; Miller, M. *J. Org. Lett.* **2010**, *12*, 392.
(14) Alder, K.; Stein, G. *Angew. Chem.* **1937**, *50*, 510.
(15) (a) Martin, J. G.; Hill, R. K. *Chem. Rev.* **1961**, *61*, 542. (b) Craig, D.; Shipman, J. J.; Fowler, R. B. *J. Am. Chem. Soc.* **1961**, *83*, 2885.
(16) (a) Sustmann, R.; Böhm, M.; Sauer, J. *Chem. Ber.* **1979**, *112*, 883. (b) Pfeffer, H. U.; Klessinger, M. *Chem. Ber.* **1979**, *112*, 890.
(17) (a) Andrews, L. J.; Keefer, L. M. *J. Am. Chem. Soc.* **1995**, *77*, 6284. (b) Holliday, R. E.; Hamer, J. *J. Org. Chem.* **1963**, *28*, 3034.
(18) Sauer, J.; Wiest, H.; Mielert, A. *Chem. Ber.* **1964**, *97*, 3183.
(19) (a) Munchausen, L. L.; Houk, K. N. *J. Am. Chem. Soc.* **1976**, *4*, 937. (b) Houk, K. N.; Loncharich, R. J.; Blake, J. F.; Jorgensen, W. L. *J. Am. Chem. Soc.* **1989**, *111*, 9172. (c) Karcher, T.; Sicking, W.; Sauer, J.; Sustmann, R. *Tetrahedron Lett.* **1992**, *33*, 8027. (d) Jorgensen, W. L.; Lim, D.; Blake, J. F. *J. Am. Chem. Soc.* **1993**, *115*, 2936. (e) Jursic, B. S. *J. Mol. Struct.: THEOCHEM* **1995**, *358*, 139. (f) Branchadell, V. *Int. J. Quantum Chem.* **1997**, *61*, 381. (g) Froese, R. D.; Humbel, S.; Svensson, M.; Morokuma, K. *J. Phys. Chem. A* **1997**, *101*, 227. (h) Froese, R. D.; Coxon, J. M.; Wesr, S. C.; Morokuma, K. *J. Org. Chem.* **1997**, *62*, 6991. (i) Coxon, J. M.; Froese, R. D.; Ganguly, B.; Marchand, A. P.; Morokuma, K. *Syn. Lett.* **1999**, *11*, 1681. (j) Aurell, M. J.; Pereze, P.; Contreras, R.; Domingo, L. R. *J. Org. Chem.* **2003**, *63*, 3884. (k) Hehre, J. W. *A Guide to Molecular Mechanics and Quantum Chemical Calculations*; Wavefunction, Inc.: Irvine, CA, 2003; p 304. (l) Domingo, L. R.; Aurell, M. J.; Perez, P.; Contreras, R. *J. Org. Chem.* **2003**, *68*, 3884. (m) Jones, G. O.; Guner, V. A.; Houk, K. N. *J. Phys. Chem. A* **2006**, *110*, 1216.
(20) (a) Yepes, D.; Donoso-Tauda, O.; Murray, J. S.; Politzer, P.; Jaque, P. *Phys. Chem. Chem. Phys.* **2013**, *15*, 7311. (b) Yepes, D.; Murray, J. S.; Domingo, L. R.; Politzer, P.; Jaque, P. *Phys. Chem. Chem. Phys.* **2014**, *16*, 6726. (c) Murray, J. S.; Yepes, D.; Jaque, P.; Politzer, P. *Comput. Theor. Chem.* **2015**, *1052*, 270−280.
(21) Frisch, M. J.; Trucks, G. W.; Schlegel, H. B.; Scuseria, G. E.; Robb, M. A.; Cheeseman, J. R.; Scalmani, G.; Barone, V.; Mennucci, B.; Petersson, G. A.; Nakatsuji, H.; Caricato, M.; Li, X.; Hratchian, H. P.; Izmaylov, A. F.; Bloino, J.; Zheng, G.; Sonnenberg, J. L.; Hada, M.; Ehara, M.; Toyota, K.; Fukuda, R.; Hasegawa, J.; Ishida, M.; Nakajima, T.; Honda, Y.; Kitao, O.; Nakai, H.; Vreven, T.; Montgomery, J. A., Jr.; Peralta, J. E.; Ogliaro, F.; Bearpark, M.; Heyd, J. J.; Brothers, E.; Kudin, K. N.; Staroverov, V. N.; Kobayashi, R.; Normand, J.; Raghavachari, K.; Rendell, A.; Burant, J. C.; Iyengar, S. S.; Tomasi, J.; Cossi, M.; Rega, N.; Millam, M. J.; Klene, M.; Knox, J. E.; Cross, J. B.; Bakken, V.; Adamo, C.; Jaramillo, J.; Gomperts, R.; Stratmann, R. E.; Yazyev, O.; Austin, A. J.; Cammi, R.; Pomelli, C.; Ochterski, J. W.; Martin, R. L.; Morokuma, K.; Zakrzewski, V. G.; Voth, G. A.; Salvador, P.; Dannenberg, J. J.; Dapprich, S.; Daniels, A. D.; Farkas, Ö.; Foresman, J. B.; Ortiz, J. V.; Cioslowski, J.; Fox, D. J. *Gaussian 09*, Revision D.01; Gaussian, Inc.: Wallingford CT, 2009.
(22) Zhao, Y.; Truhlar, D. G. *Theor. Chem. Acc.* **2008**, *120*, 215.
(23) (a) Pieniazek, S.; Houk, K. N. *Angew. Chem.* **2006**, *118*, 1470. (b) Pieniazek, S.; Clemente, F. R.; Houk, K. N. *Angew. Chem., Int. Ed.* **2008**, *47*, 7746.
(24) Barone, V.; Cossi, M. *J. Phys. Chem. A* **1998**, *102*, 1995.
(25) Cossi, M.; Rega, N.; Scalmani, G.; Barone, V. *J. Comput. Chem.* **2003**, *24*, 669.
(26) (a) Ess, D. H.; Houk, K. N. *J. Am. Chem. Soc.* **2007**, *129*, 10646. (b) Ess, D. H.; Houk, K. N. *J. Am. Chem. Soc.* **2008**, *130*, 10187. (c) Hayden, A. E.; Houk, K. N. *J. Am. Chem. Soc.* **2009**, *131*, 4084. (d) van Zeist, W. J.; Bickelhaupt, F. M. *Org. Biomol. Chem.* **2010**, *8*, 3118. (e) Liu, F.; Paton, R. S.; Kim, S.; Liang, Y.; Houk, K. N. *J. Am. Chem. Soc.* **2013**, *135*, 15642. (f) Fernández, I. *Phys. Chem. Chem. Phys.* **2014**, *16*, 7662. (g) Fernández, I.; Bickelhaupt, F. M. *Chem. Soc. Rev.* **2014**, *43*, 4953.
(27) Jencks, W. P. *Chem. Rev.* **1985**, *85*, 511.
(28) Walsh, R.; Wells, J. M. *J. Chem. Soc., Perkin Trans.* **1972**, *2*, 52.
(29) Legault, C. Y. *CYLview*, 1.0b; Université de Sherbrooke: Sherbrooke, QC, Canada, 2009; http://www.cylview.org.

DOI: 10.1021/acs.joc.5b00174
J. Org. Chem. 2015, 80, 3530−3537